

1 **Solvent, Substituents and pH Effects towards the Spectral Shifts of some highly colored**
2 **Indicators**

3 MAMDOUH S. MASOUD, REHAB M. I. ELSAMRA* and SOKAINA S. HEMDAN

4 *Department of Chemistry, Faculty of Science, Alexandria University, Alexandria, Egypt*

5
6 *Abstract:* The solvatochromic responses of six indicators namely Sudan orange, Alizarin yellow
7 R, Aurin tricarboxylic acid, Alizarin yellow GG, Titan yellow and Eriochrome black-T
8 dissolved in seven solvents of different polarities have been measured at room temperature. The
9 UV/Vis absorption spectral shifts were analyzed by multiple linear regression analysis and
10 Kamlet-Taft's equation. The observed solvatochromism was found to depend on the presence
11 of donor and acceptor substituents in the conjugated systems of the indicator and the physical
12 properties of the solvent molecules. The pH effects on the wavenumbers of the absorption band
13 maxima of some indicators with different constituents were discussed at room temperature and
14 the mechanism of ionization was explained. The dissociation constants (pK_a) of the investigated
15 compounds were precisely assessed and the existence of individual predominant ionic species
16 was assigned by constructing distribution diagrams at different pH ranges.

17
18 *Keywords:* azo dyes; solvatochromism; Kamlet-Taft parameters; acid dissociation constant.

19
20 RUNNING TITLE: AZO DYE INDICATORS

21
22 INTRODUCTION

23 Indicators are widely used in analytical chemistry for quantitative and qualitative
24 analysis.¹ Most indicators possess an azo group conjugated to one or two arenes. The presence
25 of donor and acceptor substituents in the conjugated systems of the indicator can be of interest
26 in the study of solvent and substituent effects on the UV/Vis spectroscopic absorption maxima,
27 λ_{max} , of the azobenzene dyes. Also, the planarity of the azo link contrast with the other part of
28 the system should allow larger π electron transmission and lead to higher optical activity.²
29 Application of the techniques of multiple linear regression has proved to be exotically
30 successful and has greatly improved the understanding of the solvent role.³ Besides, the
31 dissociation constant (pK_a) is an important physicochemical parameter in the biophysical
32 characterization of using azo dyes as drugs and may be helpful in predicting the behavior of a
33 drug under *in vivo* conditions.⁴

* Corresponding author. Email: rehab_elsamra@hotmail.com

34 This article is part of a continuing investigation of structural chemistry of biologically
35 active compounds containing nitroso, nitro and azo chromophoric groups.⁵⁻¹¹ Here we aimed
36 to throw light on the solvents effect on the absorption spectra of highly colored indicators
37 [Sudan orange (SO), Alizarin yellow R (AYR), Aurin tricarboxylic acid (ATA), Alizarin yellow
38 GG (AYGG), Titan yellow (TY) and Eriochrome black-T (EBT)] in the visible and UV region
39 where these compounds absorb due to extensive conjugation of the azo group with the aromatic
40 rings. Solvents are selected to show a wide variety of solvent parameters and hydrogen bonding
41 capacity to permit a good understanding of solvent-induced spectral shifts. Moreover, the UV–
42 Vis absorption spectra of some indicators were investigated in aqueous buffer solutions of
43 different pH values and used for computing the dissociation constants (pK_a). The ranges of pH,
44 where individual ionic species are predominant have been determined.

45

46

EXPERIMENTAL

Chemicals and Materials

48 All indicators and starting materials used in this work were purchased from Fluka, BDH
49 and Sigma companies. The chemical structures of the investigated indicators and their
50 abbreviations are presented in Fig. S-1 of the Supplementary material to this paper. The solvents
51 were of HPLC grade and have been used without further purification. All solutions were
52 prepared with de-ionized and CO₂-free water. The universal buffer used in this study was
53 prepared by mixing 0.04 M of H₃BO₃, H₃PO₄ and CH₃COOH acids and adding the required
54 volume of 0.2 M KOH (CO₂ free) to give the desired pH. The ionic strength of the studied
55 solution was adjusted by adding 0.5 M solution of KCl.

Procedure

57 UV/Vis absorption spectral measurements were recorded for each indicator in the
58 proper solvent with a Perkin-Elmer Lambda 19 spectrophotometer model cell covering the
59 wavelength range 200-900 nm at room temperature (~20 °C). Seven different solvents namely
60 1,4-dioxane, ethanol (EtOH), N,N-dimethylformamide (DMF), dimethyl sulfoxide (DMSO),
61 acetone, acetonitrile and water were used. These solvents have different polarity parameters (E ,
62 K , M , J , H and N), mainly related to the refractive index n and dielectric constant D of each
63 solvent.¹²⁻¹⁵ The solvatochromic parameters (π^* , α and β) were taken from literature.¹⁶ The
64 physical parameters for the solvents at 20 °C are collected in Table S-I of the Supplementary
65 material. The dissociation constants of the indicators were determined by means of the data

66 obtained in the pH range 3.0-11.5. The pH value was measured by using previously calibrated
67 MARTINI instrument pH-benchmark.

68 *Data treatment*

69 The observed peak position of an absorption band, Y , in a given solvent has been
70 expressed as a linear function using different combinations (one-, two-, three- and four) of
71 solvent polarity parameters (E, K, M, J, H and N), X_n , by Eq. 1.

$$72 \quad Y = a_o + a_1X_1 + a_2X_2 + \dots + a_nX_n \quad (1)$$

73 The regression intercept, a_o , has been assumed to be an estimate of the peak position for gas
74 phase spectra. $a_1, a_2 \dots a_n$ are the solvent polarity parameters coefficients.¹⁷ SPSS program has
75 been used to determine these coefficients by multiple regression technique. The effect of
76 specific chemical interactions (hydrogen bonding) and non-specific solvent interactions
77 (dipolarity / polarizability) on the position of UV/Vis absorption bands of the studied indicators
78 have been evaluated by using the Kamlet–Taft approach,¹⁸ (Eq. 2):

$$79 \quad \nu_{max} = \nu_{max,0} + a\alpha + b\beta + s\pi^* \quad (2)$$

80 where ν_{max} is the maximum wavenumber (cm^{-1}) of the absorption band of the indicator
81 dissolved in pure solvent. $\nu_{max,0}$ is the solute property of a reference system and represents the
82 regression intercept which corresponds to the gaseous state of the spectrally active substance.
83 α describes the HBD (hydrogen-bond donating) ability or solvent "acidity", β the HBA
84 (hydrogen-bond accepting) ability or solvent "basicity", π^* the dipolarity / polarizability of the
85 solvents. a, b & s are solvent-independent correlation coefficients that indicate the contribution
86 of each solvatochromic parameters to the UV/Vis absorption peak shift.

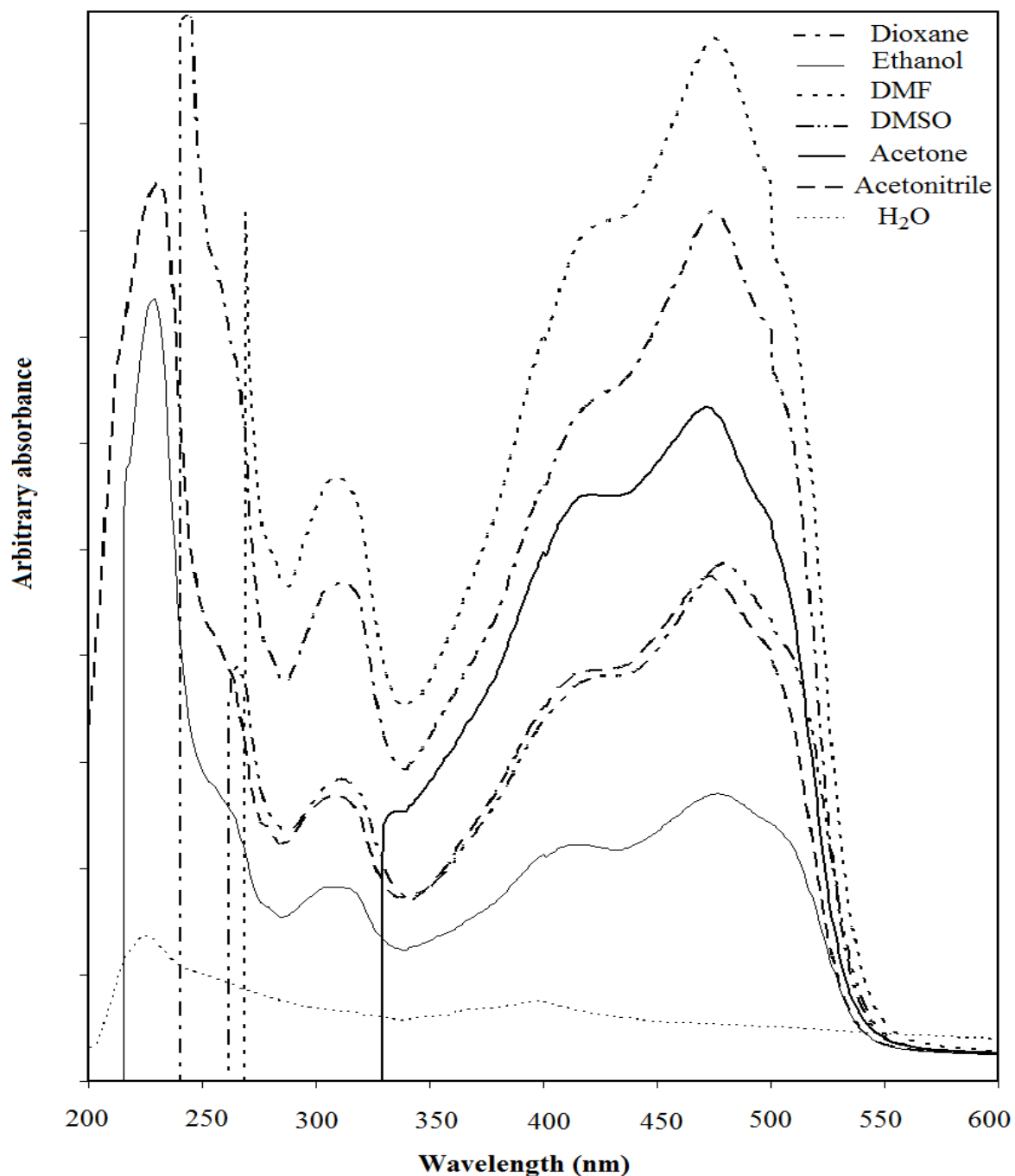
87

88 RESULTS AND DISCUSSION

89 *Solvent effects on the UV-Vis absorption spectra*

90 The electronic absorption spectra of Sudan orange (SO) in presence of different solvents
91 is selected for demonstration, Fig. 1. Different absorption bands of the investigated indicators
92 in different solvents are listed in Table I. Generally, the electronic absorption spectra of the
93 compounds in solution exhibit two types of bands. The shorter wavelength band in the UV
94 region of 247–326 nm is observed in all solvents used - except in acetone - which is ascribed
95 mainly to the π - π^* transition of the benzenoid system present in the structure of the studied

96 indicators. The second band observed in the region of 307–540 nm is assigned to $n-\pi^*$ transition
97 with a considerable charge-transfer character (CT transition). The charge-transfer nature of this
98 band is deduced from its broadness as from the sensitivity of its λ_{\max} to the type of substituent
99 attached to the azo coupler.¹⁹



100
101 Fig. 1. Electronic absorption spectra of Sudan orange in presence of different solvents.

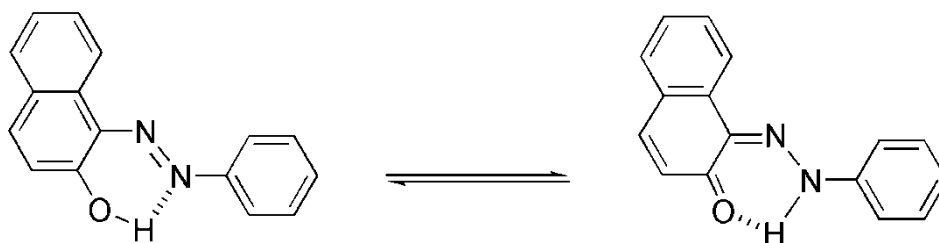
102 TABLE I. Electronic absorption spectra of the indicators in presence of different solvents (λ_{\max} , nm)

103 In addition to the lone pair of electrons of the azo group, the arene moiety of the molecules

Compounds	1,4-Dioxane	Ethanol	DMF	DMSO	Acetone	Acetonitrile	H ₂ O
EBT	287	281	274	284	-	286	278
	379	-	330	331	366	332	338
	403	394	399	398	403	400	-
	500	509	-	513	500	504	535
SO	265	259	269	266	-	260	-
	312	307	309	312	-	309	-
	414	408	424	425	412	407	395
	470	477	475	497	468	473	508
AYR	-	271	281	270	-	235	236
	290	296	308	306	-	305	301
	386	392	392	391	389	400	395
	-	-	540	-	542	-	-
ATA	-	247	-	262	-	234	239
	290	301	311	304	-	306	303
	395	392	393	398	396	400	388
	-	-	544	561	-	-	-
AYGG	262	260	270	263	-	257	259
	365	364	346	350	347	370	353
	-	-	393	-	384	-	-
TY	-	326	322	322	-	318	320
	-	412	412	418	400	400	408

104 contains different substituents possessing nitrogen, oxygen or sulphur atoms (*e.g.* NO₂, SO₃H,
 105 COOH and OH groups). For example, the region 307-370 nm is assigned to n-π* of COOH,
 106 OH and NO₂ groups (*e.g.* SO, EBT and AYGG). Bands observed at longer wavelength (*e.g.* at
 107 500 nm in EBT) is attributed to the weak forbidden n-π* transitions.²⁰ It was observed that the
 108 main bands of the compounds (SO and AYR) which are located in the range of 310–550 nm
 109 exhibit an apparent shift towards longer wavelengths in different solvents according to the
 110 sequence: 1,4-Dioxane < Acetone < Acetonitrile < EtOH < DMSO < H₂O. This shift agrees

111 with the change in the polarity of the organic solvents and could be considered as a result of
112 combination of several solvent characteristics such as polarity and hydrogen bonding.
113 Furthermore, the electronic spectra of the compound ATA in DMF and DMSO comprise a new
114 band appearing at much longer wavelength at 544 and 561 nm, respectively, Table I, owing to
115 solvated complex formation between solute molecules with DMF and DMSO molecules
116 through an intermolecular H-bonding.²¹ Moreover, the π - π^* band is red shifted when
117 proceeding from the nonpolar solvent 1,4-Dioxane (*e.g.* AYR: $\lambda_{\text{max}} = 290$ nm) to polar solvent
118 H₂O ($\lambda_{\text{max}} = 301$ nm). This red shift is mainly due to π^* orbital stabilization in polar solvents
119 more than the π orbital. All the studied indicators, except ATA, possess an azo group conjugated
120 to two arenes. The *trans* azo isomer possesses a lower steric hindrance compared to the *cis*
121 isomer with possible azo-hydrazone tautomerism.²² The following intramolecularly hydrogen
122 bonded structures are expected to be the most stable, *e.g.* SO (Fig. 2).



123
124 Fig. 2. Azo-hydrazone tautomerism of Sudan orange.

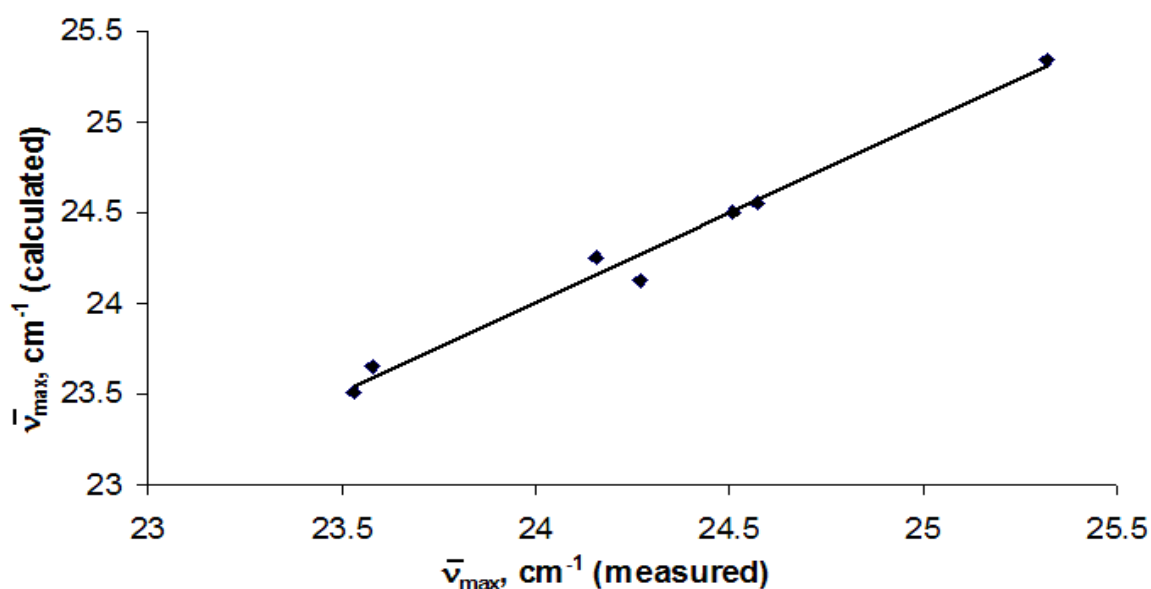
125 Regression analysis

126 Regression analysis data for Y_1 and Y_2 bands (Y_1 : $\lambda_{\text{max}} \sim 257$ to 326 nm and Y_2 : $\lambda_{\text{max}} \sim$
127 346 to 425 nm) of the investigated indicators is given in Tables S-II–S-VII of the
128 Supplementary material. A value of MCC near to unity and / or a small value (near zero) of the
129 significance parameter (P) mean the correlation is good. The analysis of the spectral shifts using
130 one-parameter equation showed that all MCC values for all solvent parameters are very poor
131 indicating difficulty of correlation for the studied spectral region Y_1 and Y_2 . However, the
132 parameter K gives a moderate correlation [MCC = 0.767, 0.640 and 0.423 for ATA, AYR and
133 TY respectively] for the region Y_1 , *i.e.* the dielectric constant (D) of the solvent is the
134 predominant parameter to explain the spectral shifts. The regression analysis of the two-
135 parameter equations improves the correlations. For instance, when the parameter E is combined
136 with the parameter M , *e.g.* SO, the MCC value jumped from 0.585 to 0.816 for the region Y_2 ,
137 Table S-II. This is probably due to the presence of the OH substituent in the ortho position of
138 the arylazo moiety which eases the formation of hydrogen bonds with the solvent.

139 For the studied spectral region Y_1 , the three-combinations (K, M, E), (K, N, E) and ($M,$
 140 N, E) for TY (SO_3H and CH_3 substituents), Table S-VII, shows better fit compared to ATA
 141 (COOH and OH substituents), Table S-IV. Also, the combinations (K, M, E), (K, N, E) and ($M,$
 142 N, E) for AYG ($m\text{-NO}_2$), Table S-V, show poor fit compared to AYR ($p\text{-NO}_2$), Table S-III.
 143 The four parameters combinations for all compounds showed the best fit of a value of MCC
 144 equals to ~ 1.000 . This leads to the assumption that the combination of different solvent
 145 parameters K, M, N and E are effective to explain the spectral shifts depending on the electronic
 146 character of the substituent and the position of this substituent in the arene moiety of the studied
 147 indicators.

148 *Kamlet and Taft method*

149 The results of the correlation of the absorption frequencies with the Kamlet–Taft
 150 solvatochromic parameters π^* , α and β using SPSS program are given in Table II, where the
 151 values of R showing the quality of the multiparametric correlation. Fig. 3 shows the relationship
 152 between the absorption maxima ($\bar{\nu}_{\text{max}}$ (calculated)) predicted by the multicomponent linear
 153 regression using the estimated $\bar{\nu}_{\text{max},0}$, a , b and s coefficients against the experimental values
 154 ($\bar{\nu}_{\text{max}}$ (measured)) for SO as a representative example.



155
 156 Fig. 3. Linear relationship between the experimental and the calculated absorption maxima ($\bar{\nu}_{\text{max}} \times 10^3$
 157 cm^{-1}) of SO indicator obtained by multilinear regression according to Kamlet-Taft's equation.

158 TABLE II. Results of the Kamlet and Taft correlation model for all indicators

Indicators	s	a	b	$\nu_{max,0}$	R
	10^3 cm^{-1}	10^3 cm^{-1}	10^3 cm^{-1}	10^3 cm^{-1}	
EBT	0.532	0.600	0.288	24.369	0.959
SO	-0.129	1.135	-1.744	24.969	0.992
AYR	-0.466	-0.180	0.419	25.698	0.537
ATA	0.056	0.401	0.222	25.050	0.784
AYGG	2.068	-0.499	1.573	25.742	0.741
TY	-0.829	-0.048	-2.120	26.430	0.967

There is a linear relationship for all samples, Fig. 3, indicating the high correlation obtained by multilinear regression according to Kamlet-Taft's equation. Also, the correlation coefficients, R , for all indicators are nearly of the same magnitude showing a high quality of the multiparametric equation (Table II). The negative sign of " b " coefficient for the indicators TY and SO shows a positive solvatochromism or bathochromic shifts of these compounds with increasing the solvent HBA "solvent basicity". The positive sign of both " s " and " a " coefficients for the indicators EBT and ATA points to the hypsochromic shifts of the studied compounds with increasing of solvent dipolarity / polarizability and solvent HBD "solvent acidity". The percentage contribution of the calculated solvatochromic parameters from the values of regression coefficients are given in Table III and Fig. 4.

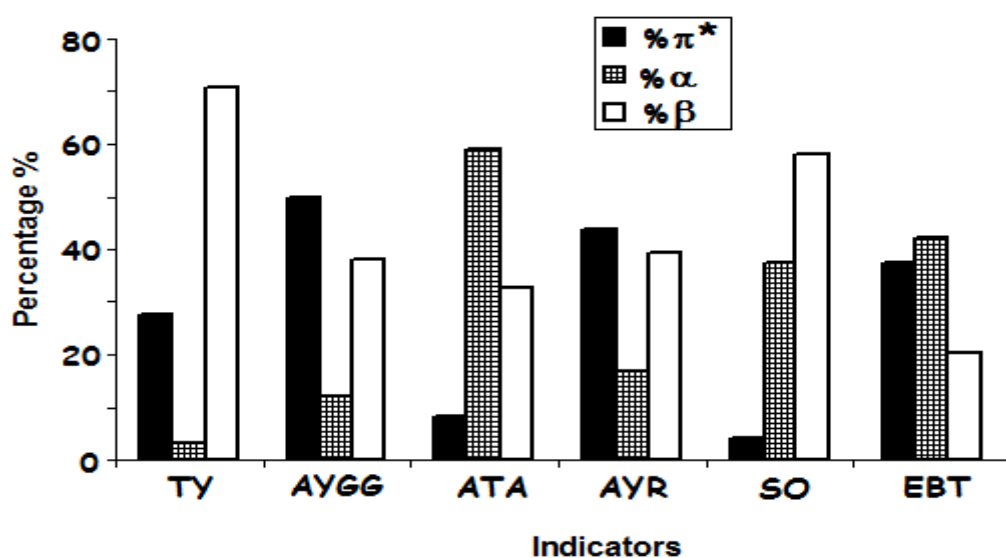


Fig. 4. Percentage contribution of the solvatochromic parameters, π^* , α and β .

TABLE III. Percentage contribution of calculated solvatochromic parameters, π^* , α and β

Indicators	% β	% α	% π^*
EBT	20.28	42.25	37.46
SO	57.98	37.73	4.29
AYR	39.34	16.9	43.76
ATA	32.70	59.05	8.25
AYGG	38.00	12.05	49.95
TY	70.74	1.60	27.66

From Table III, the solvatochromism shift arise from the hydrogen bond donating ability (α term) of the solvents is greater than the π^* and β values in case of ATA. This could be explained by the interaction of the hydrogen bonding donating solvents with the carbonyl of the three-carboxy groups of the benzene rings. However, EBT showed less HBD ability, (% $\alpha = 42.25$), compared to that observed for ATA, (% $\alpha = 59.05$), Table III. These results may be attributed to the presence of one NO_2 group in the former and three carboxy groups in the latter beside the fact that NO_2 has less hydrogen bond strength than the carboxy group.²³ The greater contribution of the HBA ability (β term) on the solvatochromism for SO suggests the existence of the OH–solvent interaction. For TY, the effect of HBD ability (α term) on the bathochromic shift is practically negligible, in contrast, the β term has a significant value, and this may be explained by the existence of two sulfonic groups together with the NH group.

Effect of pH on the electronic absorption spectra of the studied indicators

The electronic absorption spectra of the indicators under investigation at different pH's indicated that the intensity and the band position are pH dependent with the presence of some isobestic points, Fig. S-2, in the supplementary material. The isobestic point had been taken as a proof of the existence of an equilibrium between two absorbing species. The electronic spectral data at different pH's are used to compute the dissociation constant of the indicators. Three different spectrophotometric methods are applied to calculate the $\text{p}K'$ s values. The half-height,²⁴ the modified limiting absorption,²⁵ and Colleter²⁶ methods - as modified for acid base equilibrium²⁷ - gave reliance results (Table IV and Fig. 5). Different positions are available for protonation (*e.g.* $-\text{N}=\text{N}-$ to give $\text{H}-\text{N}^+=\text{N}-$). The azo-hydrazone tautomerism can be strongly influenced by synergetic tautomerism in another portion of the molecule.²⁸

TABLE IV. pK_a values of the compounds (0.5 M KCl, 20 °C)

Compound	Average pK		Colleter		Modified limiting absorption		Half height		Wave length (λ)
	pK_2	pK_1	pK_2	pK_1	pK_2	pK_1	pK_2	pK_1	
EBT	9.76 ± 0.04	6.60 ± 0.10	9.79	6.50	9.78	-	9.70	6.70	539
SO	9.51 ± 0.07	5.71 ± 0.14	9.57	5.94	9.45	5.60	9.50	5.60	521
AYGG	-	-	-	-	-	-	-	11.5	259
	-	11.1 ± 0.47	-	10.4	-	11.4	-	11.5	350
ATA	-	-	-	-	-	-	-	4.80	305
	9.48 ± 0.06	4.48 ± 0.22	9.55	4.46	9.40	4.17	9.50	4.80	224
AYR	-	11.13 ± 0.35	-	10.6	-	11.28	-	11.50	480

* Corresponding author. Email: rehab_elsamra@hotmail.com

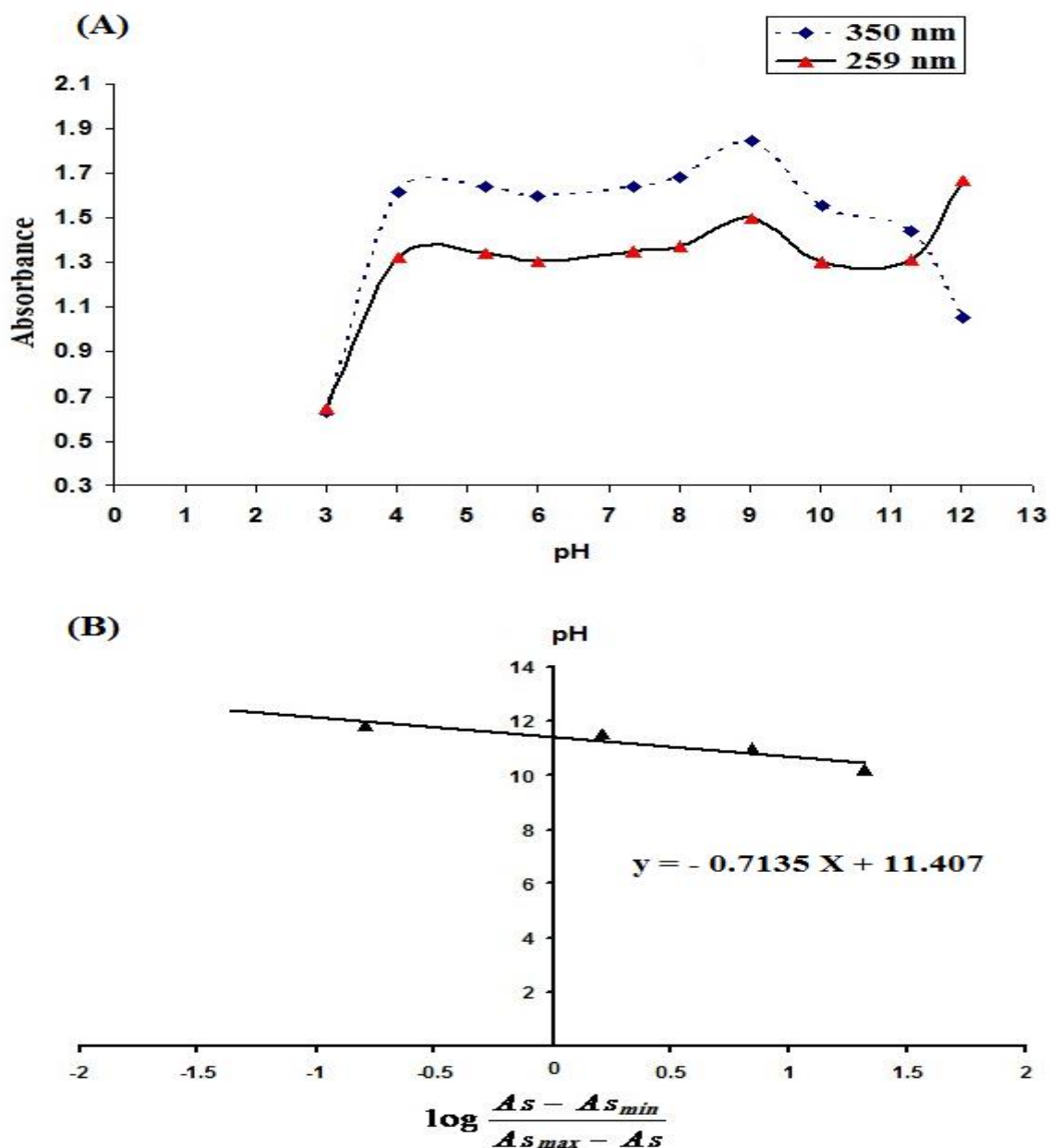
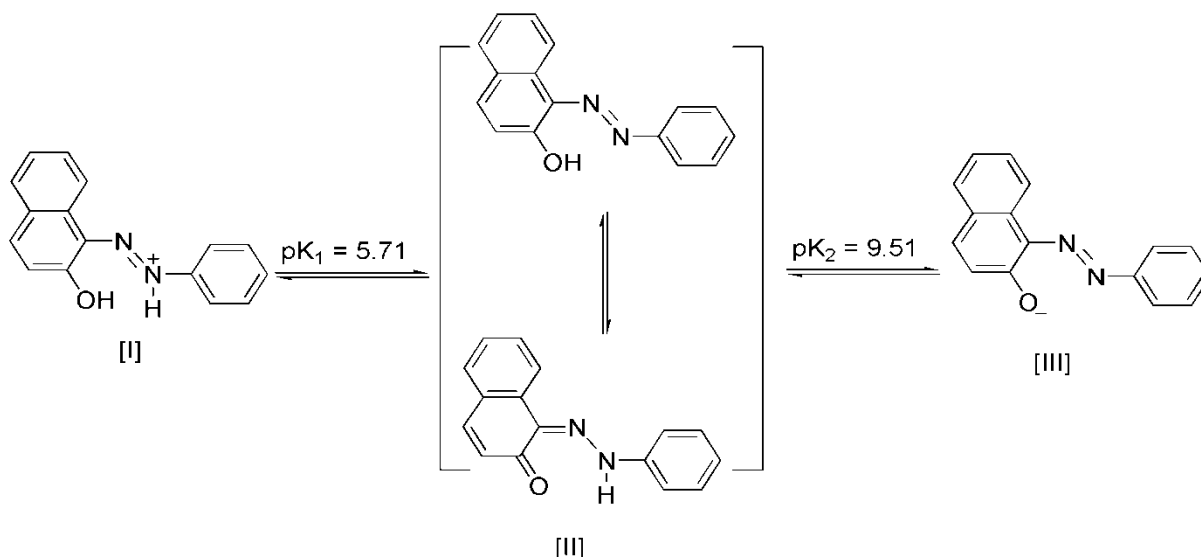


Fig. 5. (A) The half height method; Absorbance versus pH curve of AYGG at two different wavelengths ($pK_a = 11.5$), (B) Modified limiting absorption method; Log absorbance ratio versus pH of AYGG at $\lambda = 350$ nm

Sudan orange (SO) or 1-phenylazo-2-naphthol is a monoprotic dye.¹ It belongs to the azo compounds and has different possible structures in solutions. Under acidic conditions, the azo group could be protonated from the medium giving the azonium form of SO, [I]. The neutral SO can exist in azo \leftrightarrow hydrazone equilibrium, [II]. Where in alkaline solutions, SO exist as an anion, [III], Scheme 1. Calculations at 521 nm using the three mentioned spectrophotometric methods reveal two pK_a 's (5.71 ± 0.14) and (9.51 ± 0.07).

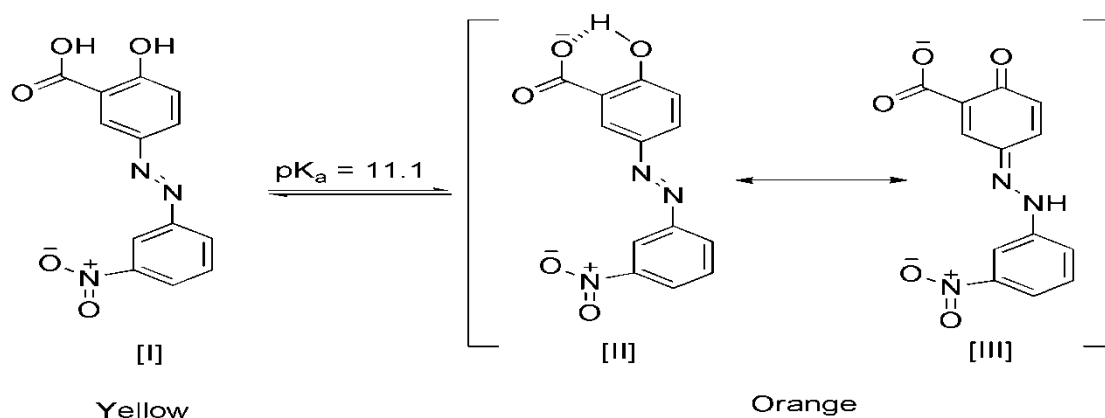
* Corresponding author. Email: rehab_elsamra@hotmail.com



Scheme 1. Cationic (I), neutral (II) and anionic (III) of SO in equilibrium with changing of pH.

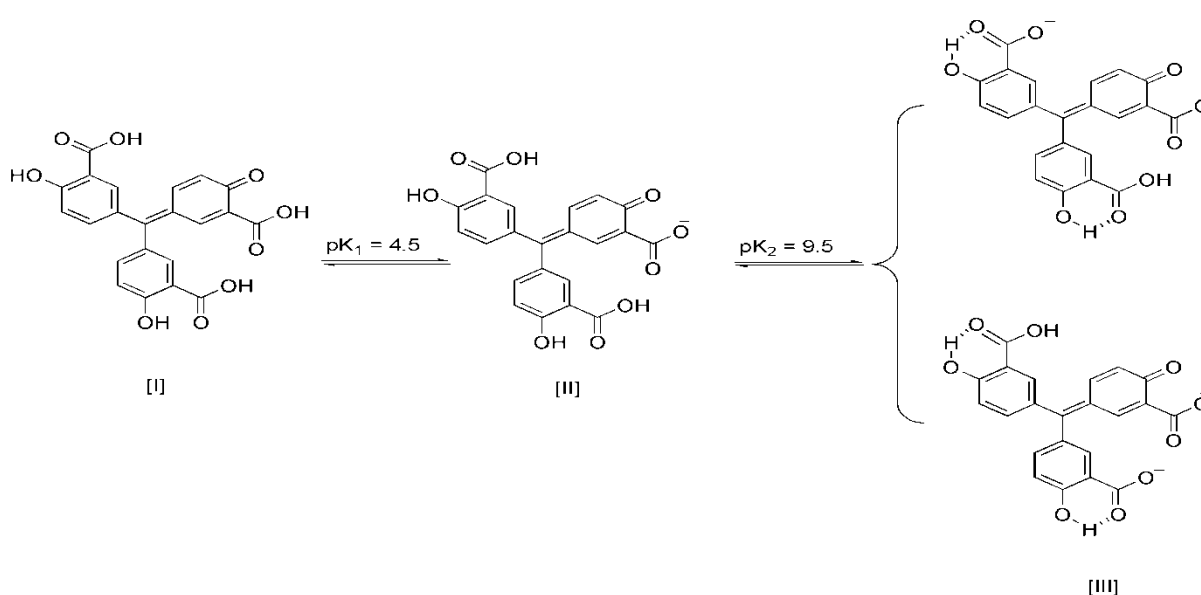
AYGG is an acid-base indicator with a dye content of 50 %. Its colour is yellow at pH = 10 and it changes to orange at pH = 12.¹ The electronic spectra of 1×10^{-4} M solution of AYGG in (50 % (v/v) ethanol – water solution) showed two well-defined bands centered at 275 nm ($\pi - \pi^*$), and at 380 nm ($n-\pi^*$ of OH group), Fig. S-2. For solutions of pH \leq 10, these two absorption bands increase stepwise in intensity with no change in position. However, these two bands are lowered in intensity and a third broad band centered at 480 nm appeared at pH \geq 11. This new band supports the formation of hydrazone form of AYGG, [III] as in Scheme 2. Calculations at 350 nm reveal only one ($pK_a = 11.1 \pm 0.47$), Table IV, which is attributed to the dissociation of the carboxylic acid group, [I]. The electron-donating OH group in the ortho position decreased the acidity of the carboxylic group lead it to ionize at pH higher than expected ($pK_a = 11.1$). AYGG is a diprotic indicator, however, the pK_2 value related to *o*-OH group is difficult to be recorded (beyond the pH range of the present study). An explanation for this difficulty is the formation of the hydrazone, [III], and the formation of the intramolecular hydrogen bond between the OH group and the COO⁻ group, [II], that decreases the ionization of the OH group.

AYR has the same chemical structure as that of AYGG except that the nitro group is in the para position to the azo link, whereas it is in the meta position in the AYGG (Fig. S-1). Despite of this difference the pK_a of AYR (11.13 ± 0.35), Table IV, is more or less the same value obtained in case of AYGG and a similar dissociation pattern for AYR is expected as in Scheme 2.



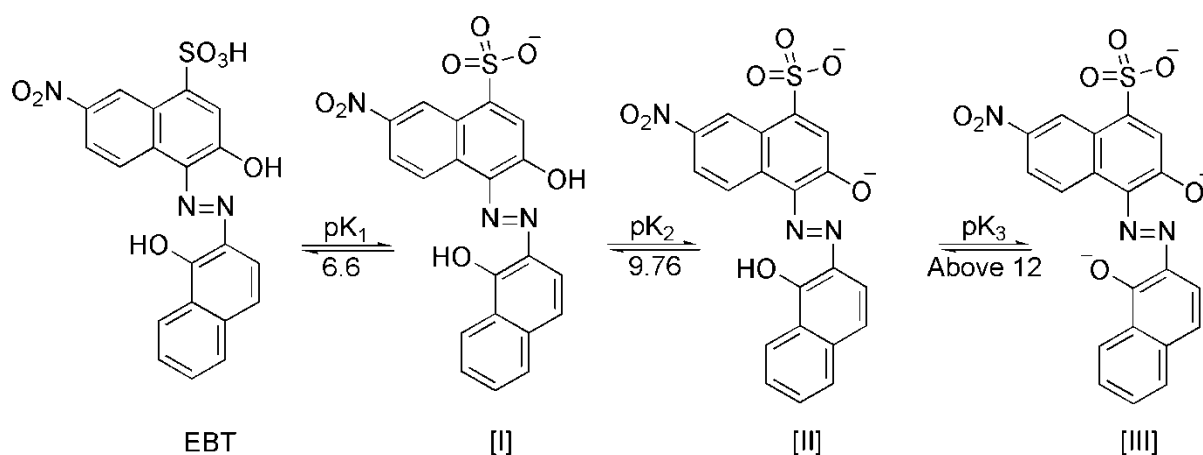
Scheme 2. Dissociation pattern of the carboxylic acid group of AYGG.

ATA is a chemical compound that readily polymerizes in aqueous solution.¹ Similar to AYGG, a third band centered at 360 nm appeared in solution of ATA at $\text{pH} \geq 11$. This could be taken as an evidence for the ionization of OH groups of ATA. Calculations at 305 nm reveal two pK_a 's, ($\text{pK}_1 = 4.48 \pm 0.22$) and ($\text{pK}_2 = 9.48 \pm 0.06$). pK_1 is attributed to the dissociation of the carboxylic acid group which is in the ortho position to the keto group, [I], Scheme 3. The electron-withdrawing keto-group in this position increases the acidity of the carboxylic group lead it to ionize at low pH. Whereas, pK_2 represents the ionization of one of the remaining carboxylic acid groups, [II], Scheme 3. The calculated number of ionized protons for the latter step was found to be ~ 0.5 indicates that this step has two different paths and suggests that the two carboxylic acid groups are not equivalent. The ionization of the OH groups of ATA may take place at pH greater than 12, beyond our study range.



Scheme 3. Suggested dissociation pattern of ATA.

EBT is a triprotic dye, in aqueous solutions, the ($-\text{SO}_3\text{H}$) proton is completely dissociated, [I], Scheme 4. The dissociation of the two hydroxyl groups of EBT takes place depending upon pH values. Calculations at 530 nm reveal only two pK_a 's (6.6 ± 0.01) and (9.76 ± 0.04). The pK_1 value (6.6) is attributed to the dissociation of the sulfonic group of the neutral form of EBT. However, the pK_2 value (9.76) is attributed to the dissociation of the OH group of the nitro-substituted naphthalene moiety, as the electron attracting nitro and sulfonic groups lowers the pK_a value. The pK_a value of the OH group of the naphthalene moiety could not be detected in our study, which suggests that its value could be above 12.²⁹



Scheme 4. Suggested dissociation pattern of EBT.

Distribution of species of AYR and SO at different pH values

In the distribution diagrams, a plot of the fraction of an acid species versus how that fraction varies with pH was made (Fig. 6). The variation of the species is due to the acid dissociation shifting as pH changes. From these diagrams, the prevailing acid species (undissociated acid or any acid anion) at any pH range could be judged. It is of interest to note that in many cases an intermediate acid anion can never be found -practically- alone at any pH range. For AYR, HA (undissociated acid species, Fig. 6A), exists predominately below $\text{pH} = 9.1$ and it is also in equilibrium with its anion form A^- as proved from the electronic spectra data. For SO (HA), the pK_1 at 5.71, Table IV, could be explained by the protonation of SO under acidic condition forming H_2A^+ (Fig. 6B). The pK_2 equals 9.51 where A^- is formed by the ionization of the OH group and reaches its maximum at $\text{pH} \sim 11.2$.

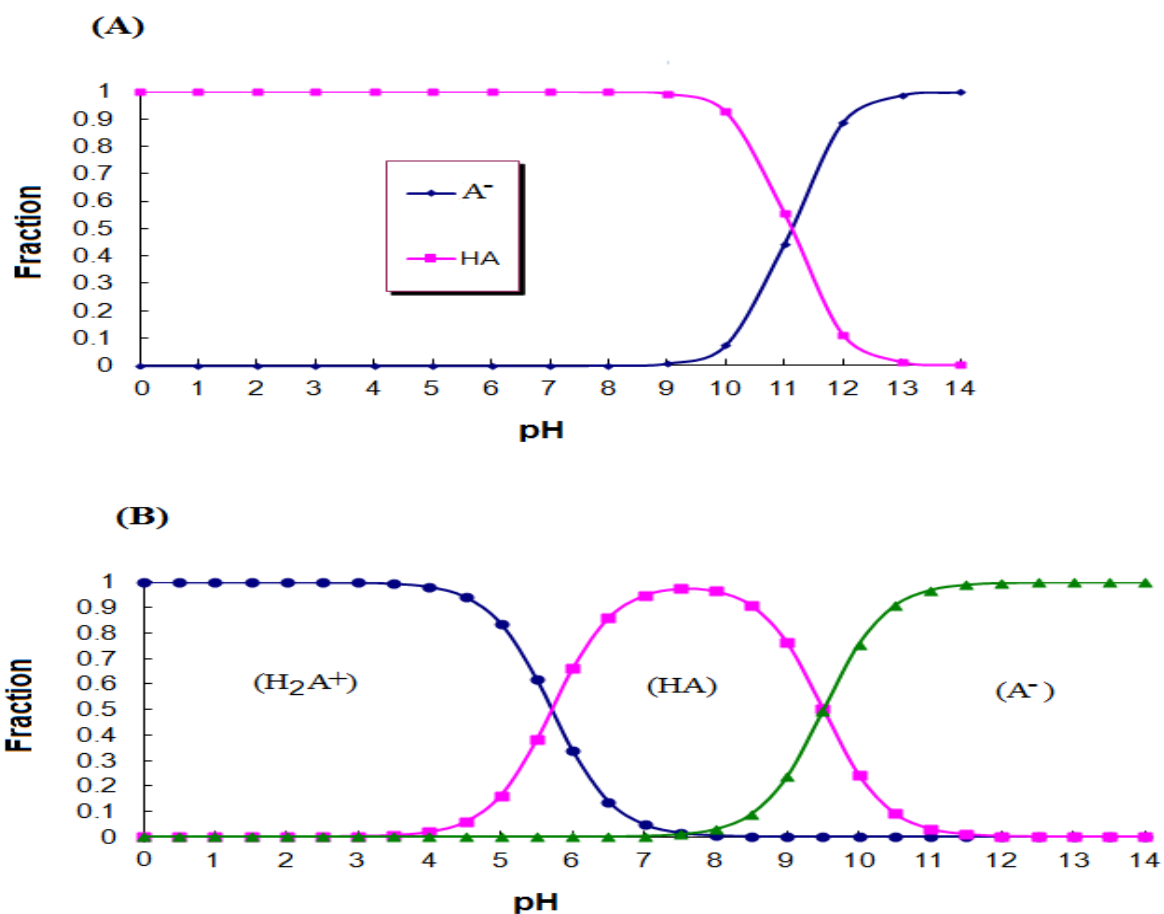


Fig. 6. Distribution diagram of the acid species of (A) AYR and (B) SO indicators at different pH's.

CONCLUSIONS

The electronic spectra of six indicators namely Sudan orange, Alizarin Yellow R, Aurin Tricarboxylic acid, Alizarin yellow GG, Titan yellow and Eriochrome black-T are affected by the nature of the solvents that differ in their properties. We can express this effect quantitatively by applying different models: mainly multiple regression and Kamlet-Taft equations. The observed solvatochromism was found to depend on the presence of donor and acceptor substituents in the conjugated systems of the indicator and the physical properties of the solvent molecules. The series of molecules studied here seem to exist in the trans azo isomer with possible azo-hydrazone tautomerism. The pH effects on the wavenumbers of the absorption band maxima of some indicators with different constituents were discussed at room temperature and the mechanism of ionization was explained. The dissociation constants (pK_a) of the investigated indicators were precisely assessed - by the described methods in this work - for the first time that is in contrast to literature where wide ranges of pH are given for their colour change.

SUPPLEMENTARY MATERIAL

The chemical structure of the studied indicators together with their abbreviations, the physical parameters for the solvents, tables containing regression data and the effect of pH spectra are available electronically from [http://www.shd.org.rs /JSCS/](http://www.shd.org.rs/JSCS/), or from the corresponding author on request.

Acknowledgements: The authors express appreciation to the Alexandria University for supporting this investigation.

ИЗВОД

НАСЛОВ РАДА

ПРВИ А. АУТОР, ДРУГИ Б. АУТОР¹ и ТРЕЋИ В. АУТОР²

Афилијација првог аутора

¹*Афилијација другог аутора*

²*Афилијација трећег аутора*

(Домаћи аутори морају доставити Извод (укључујући имена аутора и афилијацију) на српском језику, исписане ћирилицом, иза Захвалнице, а пре списка референци.) For authors outside Serbia, the Editorial Board will provide a Serbian translation of their English abstract.

REFERENCES

1. R. W. Sabnis, *Hand book of acid-base indicators*, Squire, Sanders & Dempsey LLP, San Francisco, USA, 2007
2. M. S. Zakerhamidi, M. Keshavarz, H. Tajalli, A. Ghanadzadeh, S. Ahmadi, M. Moghadam, S. H. Hosseini, V. Hooshangi, *J. Mol. Liq.* **154** (2010) 94
3. G. S. Uscumlic, J. B. Nikolic, *J. Serb. Chem. Soc.* **74** (2009) 1335
4. Y. D. Daldal, E. C. Demiralay, S. A. Ozkan, *J. Braz. Chem. Soc.* **27** (2016) 493
5. M. S. Masoud, A. M. Hindawy, M. A. Mostafa, A. M. Ramadan, *Spectrosc. Lett.* **30** (1997) 1227
6. M. S. Masoud, E. A. Khalil, A. M. Ramadan, Y. M. Gohar, A. H. Sweyllam, *Spectrochim. Acta* **67A** (2007) 669
7. M. S. Masoud, E. A. Khalil, A. M. Ramadan, S. A. Mokhtar, O. F. Hafez, *Syn. React. Inorg. Metal-Org. Nano-Metal Chem.* **44** (2014) 402
8. M. S. Masoud, A. M. Hafez, M. Sh. Ramadan, A. E. Ali, *J. Serb. Chem. Soc.* **67** (2002) 833

9. M. S. Masoud, A. M. Hindawy, A. A. Soayed, M. Y. Abd El-Kaway, *Fluid Phase Equilib.* **312** (2011) 37
10. M. S. Masoud, E. A. Khalil, S. Abou El Enein, H. M. Kamel, *Eur. J. Chem.* **2** (2011) 420
11. M. S. Masoud, A. M. Ramadan, A. A. Soayed, S. M. S. Ammar, *J. Iran. Chem. Soc.* **13** (2016) 931
12. F. W. Fowler, A. R. Katritzky, R. J. D. Rutherford, *J. Chem. Soc. B* (1971) 460
13. C. Reichardt, *Chem. Rev.* **94** (1994) 2319
14. J. G. Kirkwood, *J. Chem. Phys.* **2** (1934) 351
15. J. G. David, H. E. Hallam, *Spectrochim. Acta* **23A** (1967) 593
16. M. J. Kamlet, J. -L. M. Abboud, M. H. Abraham, R. W. Taft, *J. Org. Chem.* **48** (1983) 2877
17. L. J. Hilliard, D. S. Foulk, H. S. Gold, C. E. Rechsteiner, *Anal. Chim. Acta* **133** (1981) 319
18. R. W. Taft, J. -L. M. Abboud, M. J. Kamlet, *J. Org. Chem.* **49** (1984) 2001
19. M. Dakiky, K. Kanan, K. Khamis, *Dyes Pigm.* **41** (1999) 199
20. İ. Sıdır, E. Taşal, Y. Gülseven, T. Gungor, H. Berber, C. Öğretir, *Int. J. Hydrogen Energy* **34** (2009) 5267
21. N. M. Rageh, *Spectrochim. Acta* **60A** (2004) 103
22. A. R. Monahan, A. F. De Luca, A. T. Ward, *J. Org. Chem.* **36** (1971) 3838
23. N. Valentic, D. Mijin, G. Uscumlic, A. Marinkovic, S. Petrovic, *Arkivoc* **12** (2006) 81
24. R. M. Issa, H. Sadek, I. I. Ezzat, *Z. Phys. Chem.* **74** (1971) 17
25. A. A. Muk, M. B. Pravica, *Anal. Chim. Acta* **45** (1969) 534
26. J. C. Colleter, *Ann. Chim. (Paris)*, **5** (1960) 415
27. D. V. Jahagirdar, D. D. Khanolkar, *J. Inorg. Nucl. Chem.* **35** (1973) 921
28. P. W. Alexander, R. J. Sleet, *Aust. J. Chem.* **23** (1970) 1183
29. E. Bosch, J. Guiteras, A. Izquierdo, M. D. Prat, *Anal. Lett.* **21** (1988) 1273